

Interaction of Neopentyl Thiol with Clean and Oxygen-Modified Fe(100) Surfaces[†]

Kevin K. Meagher, Andrew B. Bocarsly, and Steven L. Bernasek*

Department of Chemistry, Princeton University, Princeton, New Jersey 08544

T. A. Ramanarayanan

Corporate Research Laboratories, Exxon Research and Engineering Company, Annandale, New Jersey 08801

Received: September 17, 1999; In Final Form: January 18, 2000

The decomposition of neopentyl thiol on clean and oxygen-modified Fe(100) surfaces has been investigated under ultrahigh vacuum conditions using temperature-programmed reaction spectroscopy, Auger electron spectroscopy, and high-resolution electron energy loss spectroscopy. On the clean Fe(100) surface upon adsorption at 100 K, the S–H and C–S bonds of the neopentyl thiol cleave, resulting in adsorbed S, H, and neopentyl alkyl fragments, in contrast to the formation of the alkyl thiolate observed on the adsorption of *n*-alkane thiols on this surface. Upon heating, some neopentyl alkyl fragments react with adsorbed surface hydrogen to evolve neopentane at 260 K. On the oxygen-modified surface, only S–H bond cleavage is observed, and a neopentyl thiolate surface species is formed. No initial neopentane evolution from the oxygen-modified surface is observed upon heating. However, on both surfaces, isobutene and trace amounts of neopentane are seen to desorb at 380 K as a result of an elimination reaction pathway for the majority of the remaining neopentyl hydrocarbon species. Small hydrocarbon fragments remain on the surface until they finally decompose to leave atomic carbon and sulfur on the iron surface at 500 K.

Introduction

In recent years, there has been much work investigating the interactions of alkane thiols with metal surfaces to produce stable adlayers. Many of these studies have been motivated by applications of industrial interest. Three of these applications are the selective C–S bond scission in the hydrodesulfurization process,¹ the use of well-defined organic films as corrosion inhibitors,² and the formation of patterned overlayers. Many studies have investigated the well-ordered adlayers formed by alkane thiols on Au surfaces.^{3–6} The hydrophobic chain–chain interactions of these adlayers induce ordering, and they have been shown to be an effective barrier to electron transport.^{7,8} Studies of the stability of these self-assembled monolayers as a function of hydrocarbon chain length indicate that longer chain thiols form overlayers that are more thermally stable due to the chain–chain interactions of the hydrocarbon tail.⁵ This property has been suggested as a basis for the mitigation of corrosion processes. Previous work has shown that it is feasible to form a chemical bond between iron and thiols if the substrate is free of oxide.⁹ Other studies have shown that thiols have been effective in inhibiting the corrosion of stainless steel in acidic media.¹⁰ However, the formation of stable thiol overlayers on iron has not been observed.

Studies of methanethiol adsorption on various metals [Pt(111),^{11,12} Cu(100),¹³ W(211),¹⁴ Fe(100),¹⁵ Ni(111),¹⁶ Ni(100),¹⁷ Ni(110),¹⁸ and Au(111)¹⁹] indicate that S–H bond cleavage occurs upon adsorption, except for the Au(111) surface where methanethiol adsorbs and desorbs molecularly. The resulting decomposition of the adsorbed methanethiol molecule varies with metal and exposure of the surface to the thiol. The interaction of various longer chain *n*-alkane thiols with the Fe-

(100) surface has also been investigated.²⁰ This work demonstrated that the adsorbed thiolate decomposed via a β -hydrogen elimination pathway at 260 K to form the resulting gas-phase alkene and a c(2×2) sulfur overlayer on the Fe(100) surface. The decomposition temperature of the thiol was independent of the adsorbed thiol chain length in contrast to desorption observations on the Au(111) system.⁵ One approach to avoiding this kinetic decomposition pathway and to perhaps stabilize the thiol overlayer on iron is to block the decomposition by substitution at the β -position. For example, methyl substitution at this carbon might enhance the thermal stability of a thiol overlayer on an iron surface. Investigating the validity of this approach is the subject of this paper.

2. Experimental Section

These experiments were performed in an ion-pumped stainless steel ultrahigh vacuum chamber. The base pressure of this system was kept below 3×10^{-10} Torr. Mounted radially on this chamber are the components to perform high-resolution electron energy loss spectroscopy (HREELS), Auger electron spectroscopy (AES), low energy electron diffraction (LEED), and temperature-programmed reaction spectroscopy (TPRS).

The Fe(100) crystal is spot-welded on two Ta wires and attached to an off-axis manipulator. By a combination of liquid nitrogen cooling and resistive heating, the crystal temperature can be adjusted between 100 and 950 K. The Fe(100) crystal was cleaned by repeated argon ion sputtering and annealing under vacuum. The surface cleanliness was verified by AES and HREELS, and the crystallographic order was verified by LEED.

Gases were introduced to the vacuum system by means of a doser attached to a Varian adjustable leak valve. The exposures were measured in langmuirs (1 langmuir = 1×10^{-6} Torr·s)

[†] Part of the special issue "Gabor Somorjai Festschrift".

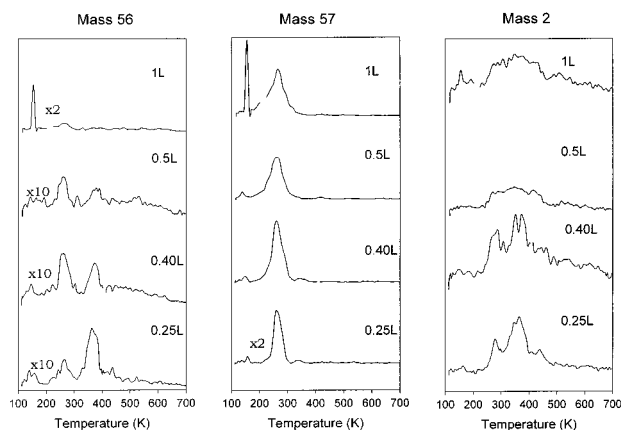


Figure 1. TPRS of neopentyl thiol on the Fe(100) surface as a function of neopentyl thiol exposure. Vertical scale expansion factors of masses 56 and 57 are referenced to mass 2.

using an ion gauge to measure total system pressure. Neopentyl thiol (API) was used as delivered following vacuum transfer and several freeze–pump–thaw degassing cycles. Deuterium (CP) was obtained from Matheson and used without further purification. Oxygen was obtained from Matheson and was also used without further purification.

TPRS measurements were carried out by positioning the Fe crystal in front of a quadrupole mass spectrometer and linearly ramping the crystal temperature at 10 K/s. The mass spectrometer ionizer is enclosed in a thin metal cylinder (2 in. diameter) with a coaxial entrance aperture of 1/4 in. diameter. This shield serves to reduce the signal from background gas desorption and to prevent electron impact on the surface. The mass spectrometer was manufactured by MKS (PPT 300em) and has a mass range of 1–300 amu. Data from the mass spectrometer is recorded on a Dell Pentium PC computer using Lab View (National Instruments) software. The temperature is regulated by a Watlow series 382 microprocessor-based temperature profiler controlling a Power Ten 0–60A power supply. The crystal is resistively heated by passing current from the controlled power supply through the tantalum mounting wires. The HREELS monochromator and analyzer were both 127° single sectors. The vibrational spectra were collected using an incident electron beam energy of 5 eV. The full width half-maximum of the elastic peak from the clean Fe(100) was typically 70 cm⁻¹. All HREELS spectra were recorded at 100 K. Data acquisition for the HREELS and AES was performed using an IBM PC-AT computer interfaced to the spectrometers. The software has been described elsewhere.¹⁵

3. Results

In the following paragraphs, the results of a series of spectroscopic measurements of neopentyl thiol adsorption and decomposition on the Fe(100) surface are presented. First, temperature-programmed reaction results are presented that indicate the overall thermal stability and decomposition mechanism of the adsorbed thiol and the products resulting from its decomposition on the clean and oxygen-modified surface. Then, overlayer composition information obtained from Auger spectroscopy is presented, which supports the decomposition mechanisms suggested by the TPRS results. Finally, vibrational spectroscopy of the overlayers is used to identify adsorbed intermediates and confirm decomposition pathways.

3.1. TPRS of Neopentyl Thiol on Clean Fe(100). Figure 1 shows the temperature-programmed reaction spectra of neopentyl thiol on the clean Fe(100) surface as a function of thiol

TABLE 1: Fragmentation of Relevant Species in Thermal Desorption Studies

species	m/e^- peak followed [shown] fragmentation pattern: m/e^- (%)
neopentyl thiol	104, [57], [41], [56] 57 (100), 41 (55.4), 55 (47.6), 29 (41.6), 104 (31), 39 (25.7), 27 (23.4), 47 (16.5), 56 (16.2), 89 (16.1)
neopentane	[57], [41], 15, [56] 57 (100), 41 (41.5), 29 (38.5), 27 (15.7), 39 (13.2), 15 (6.4), 58 (4.5), 56 (4.3), 55 (2.8), 28 (2.4)
isobutene	[56], [41] 41 (100), 56 (67.4), 39 (39.8), 55 (24.4), 28 (19.3), 27 (16.1), 29 (10.5), 40 (9.1), 53 (7.1), 50 (6.1)

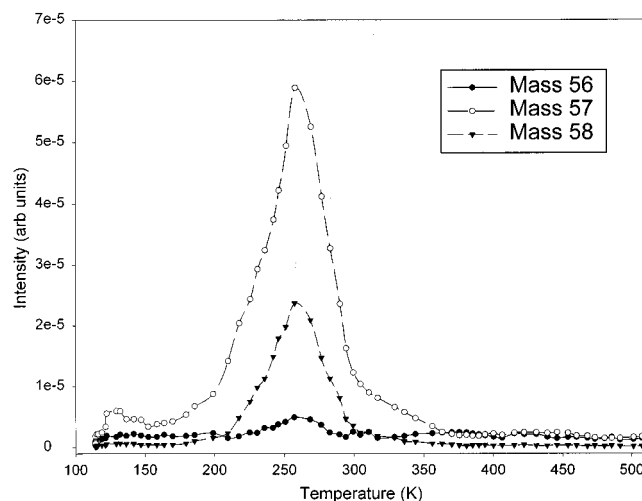


Figure 2. TPRS of neopentyl thiol on the Fe(100) surface preexposed to 150 langmuir (0.25 monolayer) of deuterium gas.

exposure ranging from 0.25 to 1.0 langmuir. Desorption spectra corresponding to m/e 56, m/e 57, and m/e 2 are shown. These masses, along with mass 18 and mass 104, were the most intense species observed and were monitored to follow the major decomposition reaction products as well as the possible desorption of the intact neopentyl thiol molecule. Table 1 summarizes the fragmentation patterns of the desorbing species. These desorbing products are highly structurally similar; therefore, assignment was based on the intensity of several masses for a given desorption peak. For example, a peak in both masses 57 and 104 was observed at 150 K. There were no further peaks in the mass 104 spectrum at higher temperature. Since only the intact molecule has a peak at mass 104, the desorption at 150 K is assigned as the intact molecule. This peak exhibits a desorption shape and behavior consistent with zero-order desorption kinetics, increasing in intensity with increasing neopentyl thiol exposure. Saturation of the Fe(100) surface sulfur coverage occurred at a 2.0 langmuir exposure based on AES measurements of surface sulfur concentration (see section 3.2), even though the intensity of the desorption peak at 150 K continued to increase for exposures greater than 2.0 langmuir. In addition to the desorption of the intact molecule at 150 K, subsequent desorptions of reaction products were also observed.

The desorption at 260 K has significant intensity in masses 57, 41, and 15, with a much smaller intensity at mass 56. On the basis of these relative intensities, this desorption is assigned to neopentane. Further studies with deuterium surface precov-
erage confirm this assignment and provide information on the mechanism of formation of this product (Figure 2). An increase in the surface concentration of hydrogen or deuterium by preexposure results in an increase in neopentane formation. Neopentane is the dominant reaction product observed during

decomposition based on analysis of all observed desorbing fragments. This neopentane desorption as illustrated by its most intense fragmentation ion, the 57 amu peak, saturates at exposures above 0.4 langmuir. Desorption intensity at mass 2 is also seen at 260 K. This peak is unambiguously assigned as desorbing H_2 . Neopentane evolution is likely to be the result of surface hydrogen and alkyl recombination. This hypothesis was examined by precovering the surface with deuterium and monitoring deuterium incorporation into the neopentane due to this recombination reaction. The results of this experiment are shown in the desorption spectra of Figure 2.

The Fe(100) surface was exposed to 150 langmuir (0.25 monolayer²¹) of D_2 , followed by exposure to 0.75 langmuir of neopentyl thiol. Similar desorption spectra were obtained with peaks at 57, 56, and 58 amu. No desorption peak was observed at 59 amu. The observation of the peak at 58/57 amu implies surface deuterium/hydrogen recombination to form the desorbing neopentane- d_1 . The initial thiol hydrogen and the precovering deuterium on the surface recombine with adsorbed neopentyl, forming both neopentane and neopentane- d_1 . There is no peak observed at mass 59, implying only a single deuterium incorporation in the desorbing product. Also observed is a decrease in the intensity of the higher temperature 56 and 57 amu desorptions as compared with the non-precovered surface.

The third desorption feature observed occurs at 380 K, with significant intensity at mass 56, 41, and 2 amu and very weak desorption at mass 57. Since mass 57 is not present in the spectra of isobutene, while mass 56 and 41 are quite significant and mass 104 is not observed at all at this temperature, the feature seen to desorb at 380 K is assigned to be predominantly isobutene. The process responsible for this desorption is most prominent at low exposures, as indicated by enhancement of all the 56 and 41 amu desorption peaks. At the same temperature, there is also a large evolution of molecular hydrogen (2 amu) due to hydrogen atom recombination. This combination of desorption peaks suggests an elimination reaction to produce surface hydrogen and the isobutene product along with the recombination of the resulting surface hydrogen to produce hydrogen and the trace amounts of neopentane. At low coverages, this elimination is most intense and declines in intensity as the exposure is increased, suggesting that the availability of open reactive sites on the surface favors the elimination product. Initial precoverage of the surface by hydrogen or deuterium suppresses the process that forms the isobutene product, favoring the lower temperature alkyl-hydrogen recombination pathway.

At 420 K, there is a final desorption of hydrogen, as well as several broad and weak desorptions of other higher masses (principally 15 and 41 amu) centered between 420 and 500 K. The HREELS data (section 3.5) indicates that there is still some hydrocarbon material present on the surface at this point, which begins to decompose to atomic S and C over this temperature range.

3.2. TPRS of Neopentyl Thiol on Oxygen-Preexposed Fe(100). Figure 3 shows the TPRS results for 0.75 langmuir exposure of neopentyl thiol to the Fe(100) surface with various oxygen precoverages. These surfaces were prepared by exposing the clean Fe(100) surface to various exposures of oxygen at 100 K, annealing to 303 K for 2 min, and then cooling to 100 K. These modified surfaces were then exposed to 0.75 langmuir of neopentyl thiol. The resulting TPRS data are strikingly different from that observed for the clean Fe(100) surface for a comparable neopentyl thiol exposure. In this case, no appreciable hydrocarbon desorption at 260 K is observed. Upon heating, a strong narrow desorption peak is observed at 150 K, with

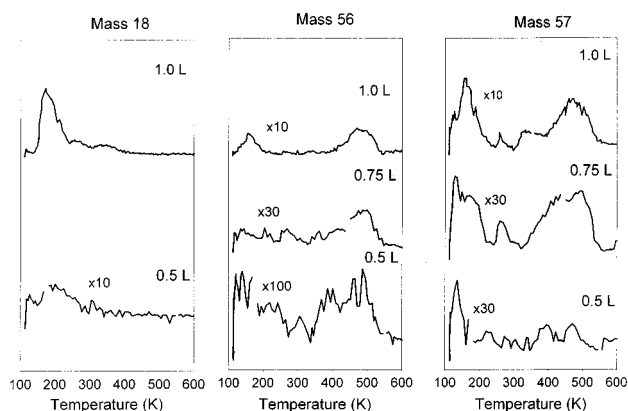


Figure 3. TPRS of 0.75 langmuir of neopentyl thiol on the Fe(100) surface preexposed to various amounts of oxygen. Vertical scale expansion factors of masses 56 and 57 are referenced to mass 18.

fragments and relative intensities again corresponding to the intact neopentyl thiol. As the temperature is increased, at 180 K molecular water is observed to desorb from the surface (mass 18). This desorption peak results from the production of water from the adsorbed surface hydrogen and the preadsorbed atomic oxygen on the surface. AES results further support this assignment. The desorption peak corresponding to neopentane, at 260 K, is not observed in this oxygen-precovered case. The only remaining desorbing hydrocarbons are observed in the TPRS for masses 56 and 57 beginning at 380 K. These desorption peaks shift to higher temperature as the oxygen preexposure is increased, until they occur at the same temperature as the total decomposition at 500 K. In these desorption peaks, mass 57 is slightly more intense than mass 56, and the peaks can be interpreted as a mixture of isobutene and neopentane based on the relative intensities of the fragment ion intensities.

3.3. AES of Neopentyl Thiol on Clean Fe(100). Following a TPRS experiment, the AES indicates that the resulting surface is constituted of iron, sulfur, and trace amounts of carbon. HREELS results for this final state (see section 3.5) indicate that atomic S and C are present on the surface [loss energies of 269 cm^{-1} ($\nu(\text{Fe}-\text{S})$) and 515 cm^{-1} ($\nu(\text{Fe}-\text{C})$)].²⁰ The amount of sulfur remaining on the surface following TPRS was determined by the Auger peak-to-peak height ratio (APPHR) of the sulfur (LMM) line at 152 eV to the iron (LMM) line at 662 eV as a function of initial thiol exposure. It has been reported previously²⁰ that the saturation S/Fe APPHR for *n*-alkane thiols on Fe(100) is 0.6. The saturation amount of sulfur on the surface for neopentyl thiol approaches this value for exposures greater than 2.0 langmuir. This corresponds to the formation of a $c(2\times 2)$ overlayer of sulfur on the iron surface following thiol decomposition.

3.4. AES of Neopentyl Thiol on Oxygen-Preexposed Fe(100). Figure 4 shows the oxygen AES (APPHR) results for 0.75 langmuir exposure of neopentyl thiol to the Fe(100) surface with various oxygen precoverages following thermal decomposition. The clean Fe(100) surface was exposed to varying amounts of oxygen at 100 K, annealed at 303 K for 2 min, then cooled to 100 K. These surfaces were then exposed to 0.75 langmuir of neopentyl thiol, heated to 900 K, and then cooled to 100 K. It has been observed previously that the Fe(100)/oxygen system upon annealing at elevated temperature results in a constant $\text{O}(510\text{ eV})/\text{Fe}(662\text{ eV})$ APPHR of 0.37.²¹ This is illustrated in Figure 4 as the horizontal dashed line and represents the equilibrium coverage of oxygen on the surface following this treatment. The decomposition of neopentyl thiol

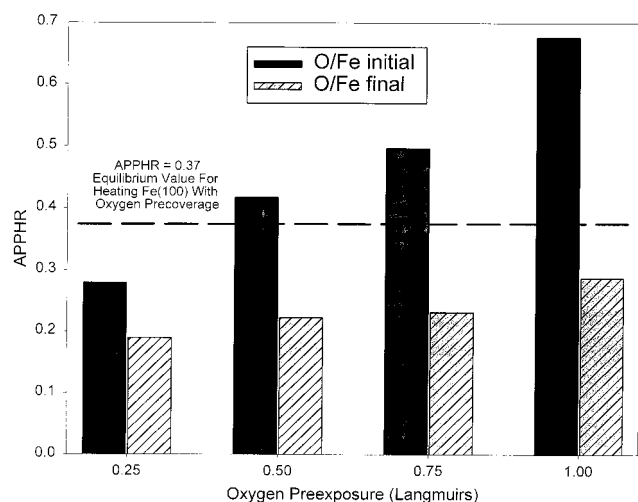


Figure 4. Auger peak-to-peak height ratios before and after thermal desorption of 0.75 langmuir of neopentyl thiol with various oxygen preexposures.

on this surface changes this system dramatically. Figure 4 demonstrates that the final oxygen APPHR in the Fe(100)/O₂/0.75 langmuir neopentyl thiol system is lower than the APPHR observed in the Fe(100)/O₂ case. This loss of oxygen suggests that an additional reactive pathway exists for the removal of oxygen. The observation of mass 18 desorption for neopentyl thiol decomposition on the oxygen-modified surface suggests water desorption via the reaction of surface hydrogen of thiol origin and preadsorbed oxygen. Additionally, it is observed that the APPHR of S(152 eV)/Fe(662 eV) is less than in the clean surface case (0.29). This indicates that less chemisorption of neopentyl thiol on this oxygen-modified Fe(100) surface occurs.

3.5. HREELS of Neopentyl Thiol on Clean Fe(100). The HREELS spectra for various exposures of neopentyl thiol to the clean Fe(100) surface are shown in Figure 5. All spectra were recorded at 100 K. The vibrational frequencies of the energy loss peaks and the peak assignments are summarized in Table 2. The peak assignments are made by comparison with the gas-phase IR of neopentyl thiol and by analogy to previous studies.²⁰

There is an intense energy loss peak observed at 2930 cm⁻¹. This peak is assigned as the $\nu(\text{C-H})$, the C-H stretching mode. The S-H stretching mode is observed at 2605 cm⁻¹ in the gas-phase spectra of neopentyl thiol; on the Fe(100) surface, it does not appear in the HREELS spectra for exposures below 1.0 langmuir. At exposures of 2.0 langmuir and higher, it is seen in the region from 2499 to 2580 cm⁻¹, indicating adsorption of the intact molecule. In the gas-phase spectra, an intense doublet is observed at 1485 and 1370 cm⁻¹, with the latter peak being more intense. These peaks are assigned to the in-phase and out-of-phase methyl C-H bending modes of the methyl groups attached to a common carbon atom. In the surface spectra, there is a broad energy loss peak observed in the range of 1430–1451 cm⁻¹, which is assigned as the unresolved methyl C-H bending modes. The loss peak at 1189–1210 cm⁻¹ is assigned as CH₂ wagging and twisting by comparison with the gas-phase spectra. The peak that occurs in the range of 906–920 cm⁻¹ is assigned as a combination of C-C stretches of a carbon center with four carbons attached. In the region from 707 to 713 cm⁻¹, a peak emerges and shifts to higher energy as the exposure is increased. This loss peak is assigned as the C-S stretch of the intact molecule. Additionally, there is a diffuse peak between 438 and 460 cm⁻¹ at low coverages that is indicative of the Fe-C stretch. This peak, coupled with the absence of the C-S

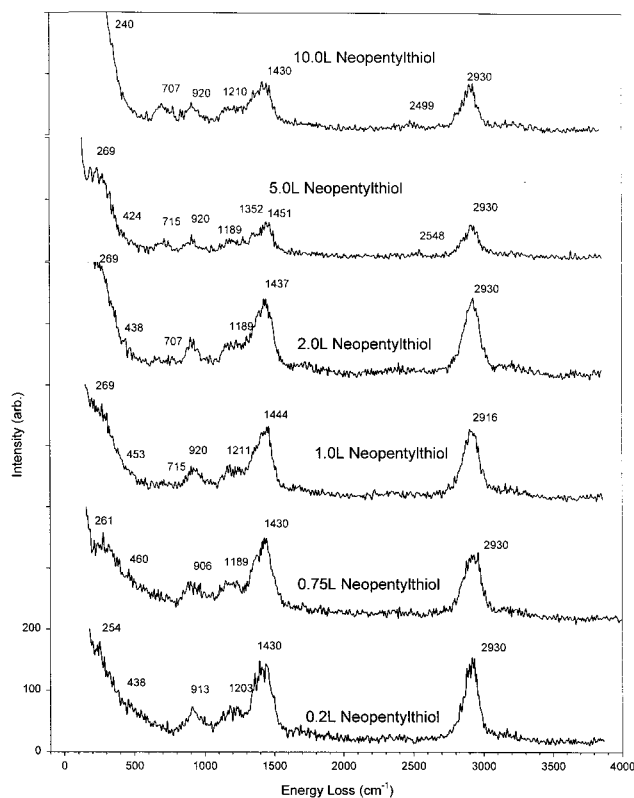


Figure 5. HREELS spectra of neopentyl thiol at various exposures at 100 K. Vibrational band assignments and energies are summarized in Table 2.

TABLE 2: Coverage-Dependent HREELS for Clean Fe(100)

vibrational mode (cm ⁻¹)	neopentyl thiol exposure (langmuir)						
	0.2	0.75	1.0	2.0	5.0	10.0	gas phase
$\nu(\text{Fe-S})$	254	261	269	269	269	240	
$\nu(\text{Fe-C})$	438	460					
$\nu(\text{C-S})$			715	707	715	707	745
$\nu(\text{C-C}) + \rho(\text{CH}_3)$	913	906	920	920	920	920	899
$\tau(\text{CH}_2) + \omega(\text{CH}_2)$	1210	1189	1211	1189	1189	1210	1192/1260
$\delta(\text{CH}_3) + \delta(\text{CH}_2)$	1430	1430	1444	1437	1451	1430	1370/1485
$\nu(\text{S-H})$					2548	2499	2605
$\nu(\text{C-H})$	2930	2930	2916	2930	2930	2930	2964

stretch at low exposures (below 1.0 langmuir), suggests C-S bond cleavage and direct interaction of the hydrocarbon fragment with the metal surface upon adsorption at 100 K at low coverages. This assignment is consistent with the mechanism suggested by TPRS for the neopentyl thiol decomposition but is in contrast to the observed behavior of the linear alkane thiols on the Fe(100) surface. The intense loss at 254–269 cm⁻¹ is assigned as the Fe-S stretch and is observed at all exposures.

Figure 6 presents the HREELS spectra for neopentyl thiol adsorbed at 100 K for an exposure of 1.0 langmuir and heated to the indicated temperatures. The indicated annealing temperatures were chosen based on the accompanying TPRS data. Vibrational energies and mode assignments are summarized in Table 3. Upon adsorption at 100 K, the HREELS spectrum shows the same features as previously assigned, except for the loss due to the S-H stretch that is too weak to be observed. After heating the crystal to 210 K, the physisorbed intact molecules have been desorbed, as is evidenced by the lack of the C-S stretch at 707 cm⁻¹. The $\tau(\text{CH}_2) + \omega(\text{CH}_2)$ modes are still present, as is the peak at 920 cm⁻¹ for the $\nu(\text{C-C})$ symmetric stretch (four C bound to a central C). After annealing to 305 K, above the major hydrocarbon desorption at 260 K, there is a significant decrease in intensity of the loss peaks above

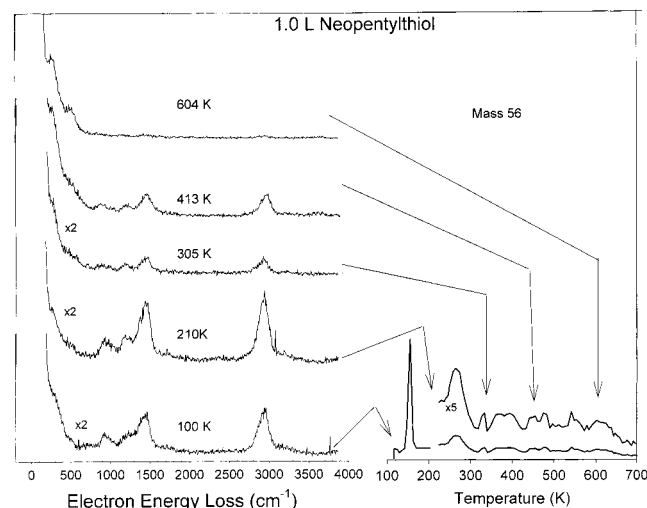


Figure 6. HREELS spectra (left panel) as a function of annealing temperature as indicated and thermal desorption spectrum of mass 56 (right panel) after the adsorption of 1.0 langmuir of neopentyl thiol at 100 K. Vibrational assignments and energies are summarized in Table 3.

TABLE 3: Temperature-Resolved HREELS Data for 1.0 Langmuir of Neopentyl Thiol on the Clean Fe(100) Surface

vibrational mode (cm^{-1})	100 K	210 K	305 K	413 K	604 K
$\nu(\text{Fe-S})$	276	261	269	261	261
$\nu(\text{Fe-C})$	481	488	481	495	495
$\nu(\text{C-S})$	707 w				
$\nu(\text{C-C}) + \rho(\text{CH}_3)$	920	920	892	892	
$\tau(\text{CH}_2) + \omega(\text{CH}_2)$	1203	1175	1189	1196	
$\delta(\text{CH}_3) + \delta(\text{CH}_2)$	1458	1437	1458	1444	
$\nu(\text{C-H})$	2945	2930	2923	2966	

500 cm^{-1} and a gain in intensity and sharpness for those below. The Fe-S stretch (269 cm^{-1}) is very much enhanced in intensity and appears more atomic in nature.²² The loss corresponding to $\nu(\text{Fe-C})$ is still diffuse; however, it increases in relative intensity. This is indicative of an iron alkyl species. The energy loss peaks above 500 cm^{-1} are diminished in intensity, and the methyl bending and stretching modes are shifted to higher energy, implying a more asymmetric adsorbed species. Additionally, the C-C stretch of the central carbon is shifted to lower energy (892 cm^{-1}), implying that the symmetry of the tertiary carbon core has been degraded. This is consistent with the shifting of the loss peaks of the methyl stretching and bending modes. Heating to 413 K, above the 380 K desorption peak assigned as isobutene, further sharpens and enhances the loss peaks assigned as $\nu(\text{Fe-S})$ and $\nu(\text{Fe-C})$. However, the most notable change is the enhancement in relative intensity of the higher energy peaks. This is indicative of the remaining surface alkyl being simpler and smaller in nature. Heating above 450 K, this remaining hydrocarbon material on the surface begins to decompose, resulting in the total decomposition of the organic material. Following heating to 604 K, only atomic S and C are left on the surface, $\nu(\text{Fe-S})$ at 261 cm^{-1} and $\nu(\text{Fe-C})$ at 495 cm^{-1} , in agreement with the AES and TPRS results.

3.6. HREELS of Neopentyl Thiol on Oxygen-Preexposed Fe(100). HREELS spectra for 0.75 langmuir of neopentyl thiol exposure to the surface with varying oxygen precoverage were also obtained (Supporting Information). Vibrational energy and mode assignments are summarized in the Supporting Information as well. As before, the clean Fe(100) surface was exposed to varying amounts of oxygen at 100 K, followed by annealing for 2 min at 303 K. Neopentyl thiol exposure was carried out

at a surface temperature of 100 K. At low preexposures of oxygen, loss peaks at 240 and 424 cm^{-1} can be distinguished and assigned as Fe-S and Fe-O, respectively. Increasing the preexposure of oxygen results in increasing the intensity and peak width of the 400 cm^{-1} peak (Fe-O). This peak dominates the low energy region of the HREELS spectra and obscures the other peaks, limiting detailed interpretation of the spectra as the preexposure increases. Additionally, the preexposure of oxygen has the effect of sharpening and intensifying the C-H and C-C modes of the adsorbed neopentyl thiol. The spectra differ from the previous clean surface spectra in that the $\nu(\text{C-S})$ stretch at $722\text{--}644 \text{ cm}^{-1}$ is readily observed. Losses corresponding to $\nu(\text{S-H})$ are not observed. This suggests that the adsorbed species is a thiolate, as was seen for the adsorption of the *n*-alkylthiols on Fe(100).²⁰ The presence of the strong $\nu(\text{C-C})$ stretch at around 900 cm^{-1} suggests that the symmetrical tertiary carbon core is intact.

Similarly, HREELS spectra for 0.75 langmuir of neopentyl thiol on the 0.25 langmuir of oxygen-preexposed surface followed by thermal decomposition were also obtained (Supporting Information). The spectra were recorded following heating to the indicated temperature and cooling to 100 K. The spectra at 110 K show features similar to the clean surface spectra, save for an intense loss at 424 cm^{-1} due to the Fe-O stretching mode and the weak loss at 679 cm^{-1} assigned to the C-S stretch. As the temperature is increased to 223 K (after intact neopentyl thiol desorption but prior to the maximum water desorption), the loss at 269 cm^{-1} grows in intensity, as do the C-H stretching and bending modes. There is a difference in the relative intensity of the 1231 cm^{-1} loss and the 1437 cm^{-1} loss. In the clean surface case, the 1400 cm^{-1} loss is much more intense; however, with oxygen preexposure, the relative intensities are more equal. This change in the relative peak intensities is similar to the spectra recorded from the clean surface after it is heated above 260 K, following the desorption of neopentane but prior to the elimination pathway. This relative intensity pattern remains intact until 373 K, corresponding to the onset of the hydrocarbon evolution seen in the TPRS from the oxygen-precovered surface. Above this temperature, the 1200 cm^{-1} loss diminishes and finally all the hydrocarbon loss peaks decrease in intensity leaving only atomic oxygen and sulfur on the surface above 523 K.

4. Discussion

4.1. Adsorption of Neopentyl Thiol on the Fe(100) Surface.

Neopentyl thiol dissociatively adsorbs on the Fe(100) surface to form surface-bound hydrogen and the neopentyl alkyl fragment at 100 K. The HREELS spectra show a lack of S-H or C-S stretches and the presence of an Fe-C stretch that support this assignment. This differs from the observation of the obvious formation of an iron thiolate in the *n*-alkane thiol interaction with the Fe(100) surface.²⁰ On the clean surface, at exposures of 2.0 langmuir or greater, a C-S stretching mode can be observed to appear and intensify corresponding to an increasing amount of the unreacted thiol on the surface. This is further supported by the presence of a weak S-H stretch at exposures greater than 2.0 langmuir. After heating above 150 K, only the partially decomposed chemisorbed species remains. The neopentyl fragment on this now sulfur- and hydrogen-modified surface is the precursor to the decomposition chemistry that follows. The maximum coverage of this species occurs at 2.0 langmuir as evidenced by AES, TPRS, and HREELS. Further exposure of neopentyl thiol results in increased intact molecule desorption and a slight increase in chemisorption until

the saturation coverage is attained at 2.0 langmuir. This exposure (2.0 langmuir) results in the same coverage of sulfur on the surface (in the final state) as in the case of *n*-alkane thiol adsorption and decomposition.²⁰ However, the exposure required to achieve this state is four times greater.²⁰

4.2. Thermal Decomposition of the Alkyl Fragment on the Clean Fe(100) Surface. At low coverages, four species are seen desorbing from the surface at differing temperatures. Initially, a small amount of intact physisorbed neopentyl thiol desorbs at 150 K. This results in an Fe(100) surface that is covered with chemisorbed alkyl fragments, hydrogen, and sulfur. At very low coverages, the alkyl fragments and the hydrogen recombine to form neopentane at 260 K. This is followed by hydrogen-hydrogen recombination occurring at 280 K. This is below the β_1 state H-H recombination temperature on clean Fe(100) at 300 K but is in agreement with the observed H-H recombination on the sulfur-modified surface from alkane thiol decomposition on Fe(100).²⁰ As the exposure of neopentyl thiol is increased, this recombination pathway continues to increase in intensity until it saturates at approximately 0.4 langmuir. The only source of hydrogen for this reaction is the thiolate hydrogen that is present on the surface at low temperature. Addition of hydrogen or deuterium prior to the exposure of neopentyl thiol increases the yield of neopentane, decreases the amount of isobutene produced, and increases the amount of desorbing hydrogen gas. With deuterium precoverage, some of the neopentane that desorbs is neopentane-*d*₁; no other deuterium incorporation is observed. This suggests that the formation of neopentane is a surface recombination that is competing with H-H recombination. The observation of H₂ desorption implies that there are some un-recombined neopentyl fragments; however, the AES results suggest that the majority of the carbon on the surface initially has desorbed by the completion of this process. This process occurs in close thermal proximity to the β_1 and β_2 state desorptions of H₂ from the Fe(100) surface.²³ This suggests that the availability of mobile hydrogen on the surface is necessary for the recombination reaction to occur. Additional support for this conclusion is the case of methane thiol on Fe(100), where alkyl hydrogen recombination is observed at 320 K to produce methane.¹⁵ Remaining after this recombination are isolated unreacted alkyl fragments surrounded by hydrogen-deficient regions of the surface. The change in relative intensity in the HREELS data further supports a large surface structural rearrangement, consistent with this conclusion.

TPRS, AES, and HREELS data support the presence of an unreacted neopentyl alkyl species on the surface at this point. This un-recombined neopentyl surface species, upon further heating, begins to undergo an elimination process to form isobutene at low coverages. Additionally, a second strong desorption of H₂ is observed coincidentally with this isobutene desorption. This H₂ desorption is broad and at a higher temperature than the H₂ desorption from the β_2 state on clean Fe(100) at 360 K,²³ suggesting that it is hydrocarbon decomposition reaction limited. As the exposure of neopentyl thiol is increased, the isobutene desorption reduces in intensity and shifts to slightly higher temperature, indicating that the elimination process is dependent on the accessibility of reactive surface sites. As the exposure is increased, the amount of sulfur remaining on the surface at this point (as evidenced by the final amount measured by AES) is quite high; hence, the prevalence of accessible active sites for elimination decreases with increasing exposure. During the elimination process, the neopentyl fragment likely loses γ -hydrogen to produce isobutene via C-C bond cleavage at the α - β position. The resulting surface

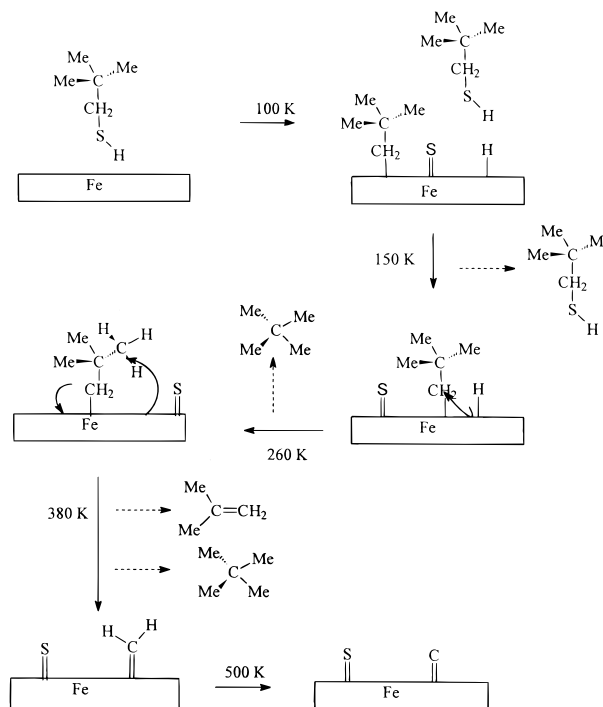


Figure 7. Proposed mechanism of adsorption, reaction, and decomposition of neopentyl thiol on the Fe(100) surface.

hydrogen can immediately recombine to form H₂ or further react with a surface-bound neopentyl to form neopentane. Neopentane formation during this process is a minor product. This type of elimination has been observed and documented for neopentyl iodide reactions on Ni.²⁴ Auger and HREELS evidence suggests that hydrocarbon material remains on the surface until it finally decomposes at approximately 500 K. HREELS spectra of this resulting species show a more asymmetric C-H stretch, a modified C-C stretch, and a more atomic Fe-C stretch. All of these observations point to a small residual hydrocarbon fragment strongly attached to the modified Fe surface as would be present in a mixed methylene surface species. At approximately 500 K, the material begins to decompose by evolving hydrogen, leaving residual atomic carbon and sulfur on the surface. The schematic in Figure 7 summarizes this sequence of events.

4.3. Thermal Decomposition of the Thiolate Species on the Oxygen-Modified Fe(100) Surface. The exposure of Fe(100) to oxygen and then subsequent heating result in a modified surface with an AES O(510 eV)/Fe(662 eV) APPHR of 0.37. However, the Fe(100) surface preexposed to oxygen followed by neopentyl thiol exposure results in surfaces with oxygen APPHRs less than 0.37. Additionally, the S(152 eV)/Fe(662 eV) APPHR is less than on the clean Fe(100) given the same exposure. The HREELS data for the oxygen-modified Fe(100) surface followed by neopentyl thiol exposure show an energy loss assigned as the ν (C-S) stretch at temperatures above the intact molecule desorption. This energy loss is not seen on the clean Fe(100)/neopentyl thiol system. The presence of an intact C-S bond above the molecular desorption temperature is indicative of thiolate formation. Oxygen preexposure of the Fe(100) is a known way to passivate the reactivity of the surface.²¹ The lowering of the surface reactivity to the surface alkyl formation explains why the C-S bond remains intact in the oxygen-modified case, thus forming the thiolate species. Additionally, it has been demonstrated in this study that oxygen scavenges surface hydrogen, desorbing molecular water and yielding a lower oxygen coverage at the completion of the

reaction. This process plays a large role in the decomposition of neopentyl thiol on the oxygen-modified Fe(100) surface. Surface hydrogen is necessary for the low-temperature decomposition pathway of hydrogen recombination on the clean surface, to form neopentane at 260 K. In the case of oxygen preexposure, this surface hydrogen reacts with oxygen to desorb water. This reactive pathway for the removal of surface hydrogen stabilizes the neopentyl thiolate. Thus stabilized, the neopentyl thiolate cannot decompose until the γ -elimination pathway is available at 380 K. Increasing oxygen exposure further passivates the surface to this elimination process. Increasing oxygen exposure increases the temperature of the onset of the evolution of the elimination product isobutene. This increasing temperature shift is capped by the total decomposition process at 500 K.

5. Conclusion

This study was initiated to probe the mechanism of thiol decomposition on the clean and oxygen-modified Fe(100) surfaces in the case in which the availability of the β -hydrogen elimination pathway present in *n*-alkane thiols is blocked. This pathway is active in the linear molecules at 260 K. In contrast to the mechanism of decomposition of *n*-alkane thiols on Fe(100), neopentyl thiol dissociatively adsorbs on the clean Fe(100) surface to produce surface hydrogen, sulfur, and a neopentyl moiety at 100 K at low coverages. The surface is saturated by exposures of 2.0 langmuir. Increased exposure results in only increased intact molecular desorption. Upon initial heating, physisorbed neopentyl thiol desorbs at 150 K. Further heating induces alkyl-hydrogen recombination and hydrogen-hydrogen recombination at 260 K to produce neopentane and hydrogen desorption products. The residual surface alkyl undergoes an elimination reaction at 380 K, yielding a mixed surface methylene-like species and gas-phase isobutene. The remaining surface hydrocarbon decomposes to surface-bound sulfur and carbon at 500 K, evolving H₂ gas in a broad desorption feature. Oxygen preexposure results in two effects: passivation of the overall surface reactivity and the low-temperature removal of surface hydrogen. The addition of a reactive pathway to remove surface hydrogen prior to hydrogen-alkyl recombination preserves the surface alkyl species until the elimination reaction at 380 K. This is demonstrated by the mitigation of the low-temperature hydrogen recombination pathway to form neopentane. The reduction of the Fe(100) surface reactivity by oxygen preexposure is seen in two ways. First, the amount of neopentyl thiol that is able to chemisorb is reduced as compared to the clean surface. Additionally, the γ -elimination process occurs at increasingly higher temperatures as the oxygen preexposure is increased.

Despite blocking the β -hydrogen elimination pathway, the overall thermal stability of the system was not significantly increased. Although there are hydrocarbon fragments and reactions present on the surface up to temperatures of 500 K, the effective coverage on the surface at these temperatures is quite low. Over 80% of the carbon initially adsorbed on the surface has desorbed by 300 K. Although the β -elimination

pathway has been mitigated, new pathways have been opened that allow the adsorbed molecule to begin decomposition at comparable temperatures. As well, on oxygen-modified surfaces where the thiolate stability is enhanced, overall thiol coverage is limited by oxygen, resulting in no significant improvement in possible corrosion inhibition by the adsorbed thiol.

Acknowledgment. This work was supported by the Department of Energy. We thank Professor Jeffrey Schwartz for useful discussions.

Supporting Information Available: Two figures and two tables are available as Supporting Information (4 pages). Figure S-1 shows HREELS spectra of 0.75 langmuir of neopentyl thiol for various preexposures of oxygen at 100 K. Vibrational assignments and energies are summarized in Table S-1. Figure S-2 shows HREELS spectra as a function of annealing temperature as indicated, after the adsorption of 0.25 langmuir of oxygen followed by 0.75 langmuir of neopentyl thiol on the Fe(100) surface. Vibrational assignments and energies are summarized in Table S-2. This material is available free of charge via the Internet at <http://pubs.acs.org>.

References and Notes

- (1) Schuman, S. C.; Shalit, H. *Catal. Rev.—Sci. Eng.* **1970**, *4*, 245–318.
- (2) Swallen, J. D.; Allara, D. L.; Andrade, J. D.; Chandross, E. A.; Garoff, S.; Israelachvili, J.; McCarthy, T. J.; Murray, R.; Pease, R. F.; Rabolt, J. F.; Wynne, K. J.; Hu, H. *Langmuir* **1987**, *3*, 932–950.
- (3) Strong, L.; Whitesides, G. M. *Langmuir* **1988**, *4*, 546–558.
- (4) Whitesides, G. M.; Laibinis, P. E. *Langmuir* **1990**, *6*, 87–96.
- (5) Bain, C. D.; Troughton, E. B.; Tao, Y. T.; Evall, J.; Whitesides, G. M.; Nuzzo, R. G. *J. Am. Chem. Soc.* **1989**, *111*, 321–335.
- (6) Dubois, L. H.; Zegarski, B. R.; Nuzzo, R. G. *J. Chem. Phys.* **1993**, *98*, 678–688.
- (7) Porter, M. D.; Bright, T. B.; Allara, D. L.; Chidsey, C. E. D. *J. Am. Chem. Soc.* **1987**, *109*, 3559–3568.
- (8) Chidsey, C. E. D.; Loiacono, D. L. *Langmuir* **1990**, *6*, 682–691.
- (9) Volmer-Uebing, M.; Stratmann, M. *Appl. Surf. Sci.* **1992**, *55*, 19–35.
- (10) Saleh, J. M.; Al-Haidari, Y. K. *Bull. Chem. Soc. Jpn.* **1989**, *62*, 1237–1245.
- (11) Koestner, R. J.; Stohr, J.; Gland, J. L.; Kollin, E. B.; Sette, F. *Chem. Phys. Lett.* **1985**, *120*, 285–291.
- (12) Rufael, T. S.; Koestner, R. J.; Kollin, E. B.; Salmeron, M.; Gland, J. L. *Surf. Sci.* **1988**, *297*, 272–285.
- (13) Sexton, B. A.; Nyberg, G. L. *Surf. Sci.* **1986**, *165*, 251–267.
- (14) Benziger, J.; Preston, R. E. *J. Phys. Chem.* **1985**, *89*, 5002–5010.
- (15) Albert, M. A.; Lu, J. P.; Bernasek, S. L.; Cameron, S. D.; Gland, J. L. *Surf. Sci.* **1988**, *206*, 348–364.
- (16) Castro, M. E.; White, J. M. *Surf. Sci.* **1991**, *257*, 22–32.
- (17) Castro, M. E.; Ahkter, S.; Golchet, A.; White, J. M. *Langmuir* **1991**, *7*, 126–133.
- (18) Huntley, D. R. *J. Phys. Chem.* **1989**, *93*, 6156–6164.
- (19) Nuzzo, R. G.; Zegarski, B. R.; Dubois, L. H. *J. Am. Chem. Soc.* **1987**, *109*, 733–740.
- (20) Cheng, L.; Bocarsly, A. B.; Bernasek, S. L.; Ramanarayanan, T. A. *Langmuir* **1994**, *10*, 4542–4550.
- (21) Lu, J.-P.; Albert, M. R.; Bernasek, S. L. *Surf. Sci.* **1989**, *215*, 348–362.
- (22) Lu, J.-P.; Albert, M. R.; Chang, C. C.; Bernasek, S. L. *Surf. Sci.* **1990**, *227*, 317–324.
- (23) Bozso, F.; Ertl, G.; Grunze, M.; Weiss, M. *Appl. Surf. Sci.* **1977**, *1*, 103–108.
- (24) Zaera, F.; Tjandra, S. *J. Am. Chem. Soc.* **1996**, *118*, 12738–12746.